APPENDIX I

APPENDIX I

UNIVERSITY OF
Miami
SCHOOL OF MEDICINE

Department of Dermatology and Cutaneous Surgery
Wound Healing Research Laboratory

Preliminary Study Report

To determine the effect of a magnetic field device
on second-degree burn wounds in a porcine model.

February 19, 2004

INVESTIGATORS AND TESTING FACILITY

Stephen C. Davis
Research Assistant Professor

Joseph A. Barbercheck
Research Associate

Carlos A. Ricotti Jr., M.D.
Research Fellow

University of Miami
School of Medicine
Department of Dermatology
& Cutaneous Surgery
P.O. Box 016250 (R-250)
Miami, Florida 33101

SPONSOR

Advatech Corp.
1 Clearlake Center, Suite 1504
250 Australia Ave S.
W. Palm Beach 33401

SPONSOR REPRESENTATIVE

Michael Spiegel, Ph.D.
Vice President

INSTITUTIONAL POLICIES AND REGULATIONS

The following experiment was submitted for approval by University of Miami's Animal Use Committee. This study was conducted in compliance of the University of Miami's Department of Dermatology & Cutaneous Surgery's Standard Operating Procedures (SOPs). The animal was monitored daily for any observable signs of pain or discomfort. In order to help minimize possible discomfort, an analgesic patch (Duragesic™ - fentanyl transdermal system: 25 μg/hr) was used on the animal throughout the study.

OBJECTIVE

The purpose of this study was to examine the effect of applied magnetic fields on the healing of non-debrided second-degree burn wounds *in vivo*. Two white specific pathogen free (SPF) pigs were selected as our experimental animals because of the morphologic and functional similarity of procine skin to human skin.

MATERIALS AND METHODS

Experimental Animals

Two young female specific pathogen free (SPF: Ken-O-Kaw Farms, Windsor, IL) pig weighing 30 kg was kept in house for one month prior to initiating the experiment. When the experiment was initiated both animals weighed 50 kg each. The animals were fed a basal diet *ad libitum* and housed individually in our animal facilities (meeting USDA compliance) with controlled temperature (19-21°C) and lighting (12h/12h LD).

Wounding Technique

The experimental animals were clipped with standard animal clippers on the day of the experiment. The skin on the back and both sides of the animals was prepared for wounding by washing with a non-antibiotic soap and sterile water. Antiseptics were not used because of their

potential effect on the healing process. The animals were anesthetized intramuscularly with ketamine HCl (20 mg/kg), xylazine (2 mg/kg) and atropine (0.05 mg/kg), followed by mask inhalation of an isoflurane and oxygen combination. Five specially designed cylindrical brass rods weighing 358g each were heated in a boiling water bath to 100°C. A rod was removed from the water bath and wiped dry before it was applied to the skin surface to prevent water droplets from creating a steam burn on the skin. The brass rod was held at a vertical position on the skin (six seconds), with all pressure supplied by gravity, to make a burn wound 8.5 mm diameter x 0.8 mm deep. Immediately after burning, the roof of the burn blister was removed with a sterile spatula. The burn wounds were made approximately 2 cm from each other.

Burn wounds pattern (Day 0)

Thirty-seven (37) burn wounds were made on the anterior two-thirds of the animal. The posterior third of the animal cannot be used because of anatomical differences in burn wound healing (a more rapid healing of burns wounds has been seen there). Burn wounds were randomly assigned to one of the following treatment groups according to the following experimental design:

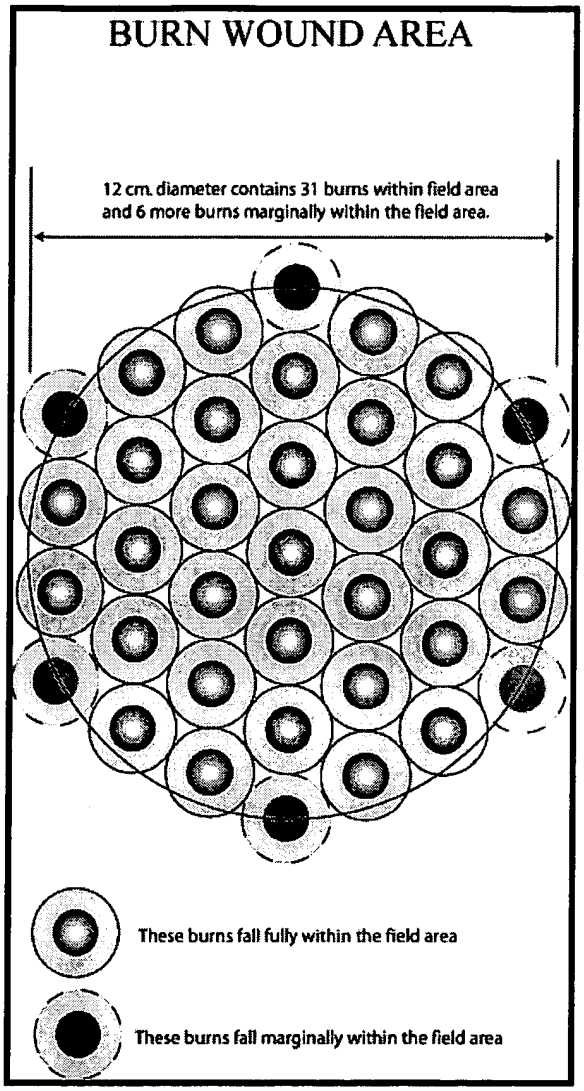

Number of Animals:

2

Treatment Groups:

A: active magnetic field
B: Untreated air exposed

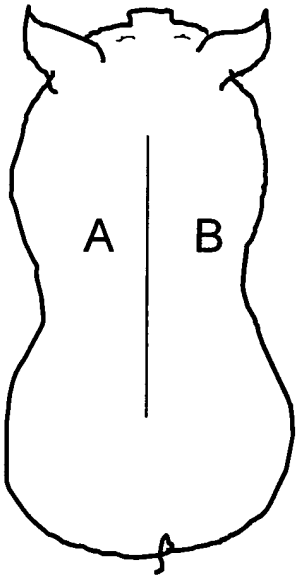

Burn Wounds:

Both A and B reflect the diagram at left, provided by sponsor

- Wounds were treated once per day for 1.5 hours on each of the first five days with the magnetic field apparatus supplied by the sponsor.
- **Note:** A total of 5 wounds per treatment group were assessed each day.

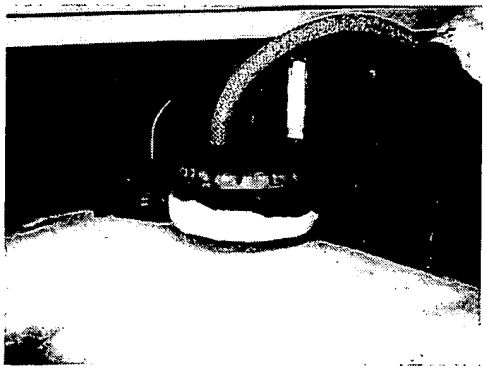

EPIDERMAL MIGRATION ASSESSMENT

Beginning on Day 8 after wounding (Day 0) and each day thereafter until all wounds were 100% completely epithelized, 5 burn wounds and the surrounding normal skin from each treatment area was excised using an electrokeratome (Figure 1-A). Any specimens that were not excised intact were discarded. The excised wounds and the surrounding normal skin were incubated in 0.5 M NaBr for 24 hours at 37°C (Figure 1-B). After incubation the specimens were separated into epidermal and dermal sheets using a salt split technique (Figures 1-C,D). The epidermis was examined macroscopically for defects in the area of the burn wounds. Epithelization was considered complete (healed) if no defect(s) were present; any defect(s) in the wound area indicated that healing was incomplete. The epidermal sheet was placed on cardboard for a permanent record.

OBSERVATIONS

There were no signs of erythema or infection in any the treatment groups. Minor appreciable differences were seen macroscopically during the treatment period. Wounds on the treated side appeared to be slightly more concaved than their counterparts in the untreated group; this observation was recorded on days four (4) and five (5).

RESULTS

The number of wounds healed (completely epithelized) was tabulated and divided by the total number of wounds sampled per day and multiplied by 100 to give a percentage of wounds completely epithelized (Table 1). The percentage of wounds healed was then plotted against

days after wounding (Figure 2). Since this is a preliminary study, statistical analysis was not performed. In order to obtain statistical results, a total of 30-40 wounds per treatment per day are required.

Days 8,9 and 10

None of the wounds from any of the treatment groups were healed (completely epithelized) at this assessment day.

Day 11

One (1) out of 10, or 10%, of the wounds from the active treatment group was healed (completely epithelized) at this assessment day.

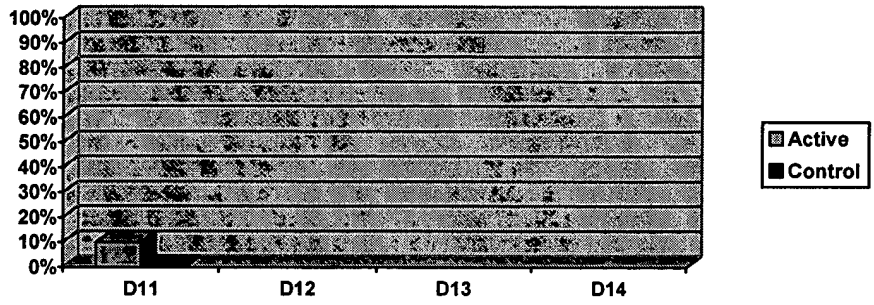

Day 12

Nine (9) out of ten (10), or 90%, of the wounds from the active treatment group were completely re-epithilized. One (1) out of ten (10), or 10%, of the wounds from the untreated group were completely epithilized.

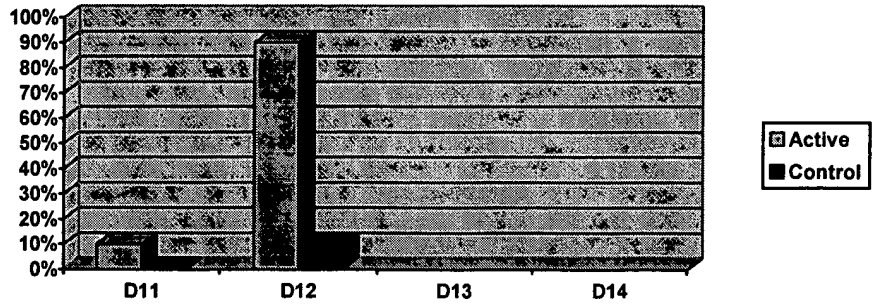

Day 13

The active treatment group remained at 100% completely epithelization and the control wounds were 50% completely epithelized.

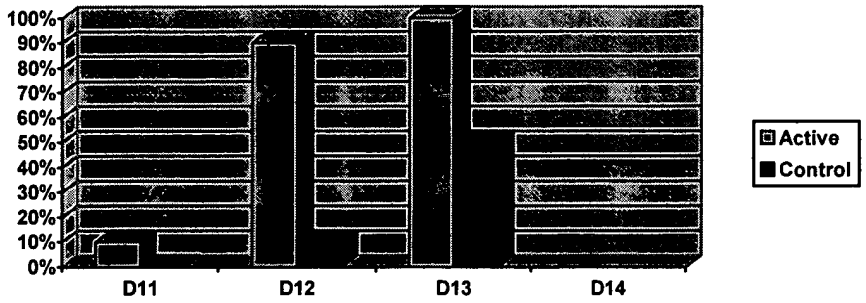

Day 14

Active wounds remained at 100% complete epithelization as compared to control wounds which were 80% completely epithelized.

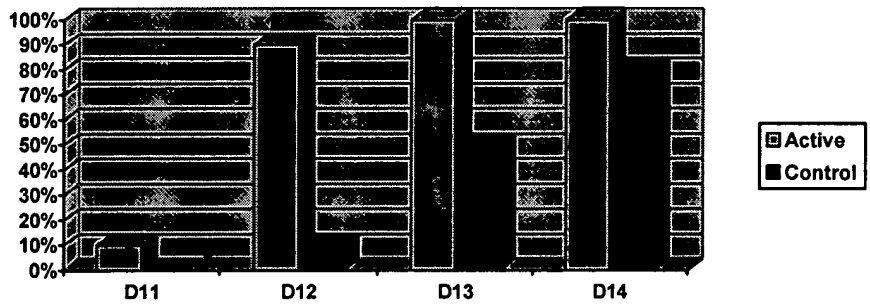

CONCLUSIONS

The magnetic field appeared to accelerate the rate of epithelization of second-degree burn wounds as compared to untreated air exposed. The magnetic field initiated complete epithelization at Day 11, one day prior to the initiation of reepithelization in untreated wounds (Day 12). In this study analyzing 2 animals, 10 wounds per treatment group per time point, the treated group demonstrated 100% re-epithelization at least 3 days before 100% reepithelization

of the untreated group. Although it appears that the magnetic fields stimulated healing of these wounds, additional animals would be needed to demonstrate a statistically significant difference between the two treatment groups.

The data from this pilot study is promising. However, the design of a more refined and space efficient device would make treatments easier especially in the clinical setting.

Table 1: Epithelization results*

Animal 1

	D8	D9	D10	D11	D12	D13	D14
Active	0/5	0/5	0/5	0/5	5/5	5/5	5/5
Control	0/5	0/5	0/5	0/5	0/5	3/5	4/5

Animal 2

	D8	D9	D10	D11	D12	D13	D14
Active	0/5	0/5	0/5	1/5	4/5	5/5	5/5
Control	0/5	0/5	0/5	0/5	1/5	2/5	4/5

Combined data (2 animals)

	D8	D9	D10	D11	D12	D13	D14
Active	0/10 (0%)	0/10 (0%)	0/10 (0%)	1/10 (10%)	9/10 (90%)	10/10 (100%)	10/10 (100%)
Control	0/10 (0%)	0/10 (0%)	0/10 (0%)	0/10 (0%)	1/10 (10%)	5/10 (50%)	8/10 (80%)

* Data is presented as the number of wounds completely epithelized over the total number of wounds assessed.

( ) Percent of wounds completely epithelized

Figure 1: Epidermal Migration Assessment

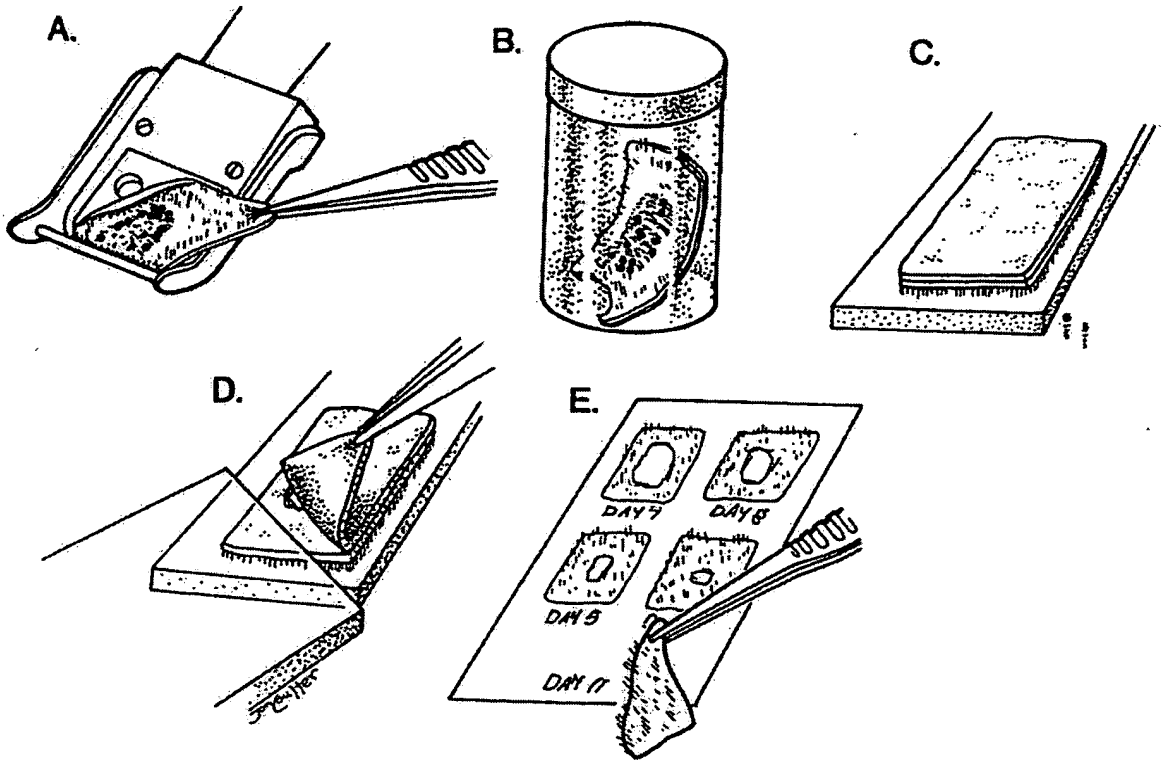

A: wound being excised
B: specimen placed in sodium bromide for separation
C: specimen placed on glass slide for separation
D: specimen being separated
E: epidermal specimens being placed on cardboard for a permanent record.

Figure 2: Epithelization results*

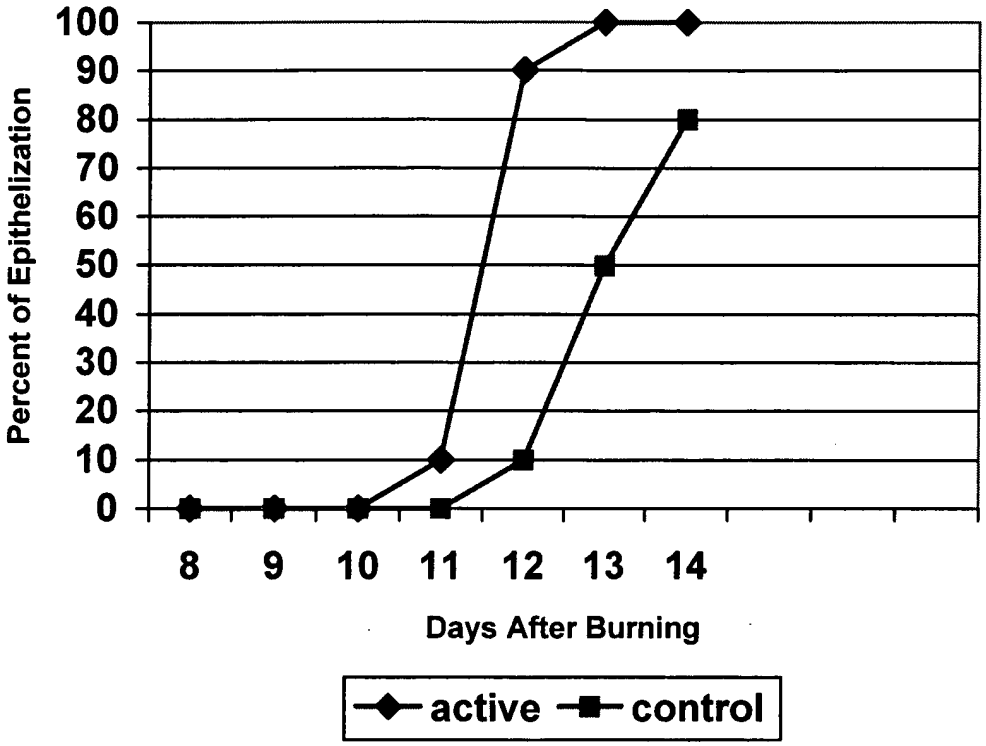

- Data is plotted as the percent of wounds completely epithelized (y-axis) vs. the days of assessment (x-axis).

Non-invasive electric magnetic field: Effects on keratinocyte migration and proliferation

Jie Li*, Ran Huo, Qianli Ma, James J. Wu, Juan Chen, Maria E. Miyar, Stephen Davis

Department of Dermatology and Cutaneous Surgery, University of Miami School of Medicine, Miami, Florida 33136

Acknowledgement:

This work was supported partially by research grants from Dermatology Foundation of South Florida (Jie Li).

***Correspondence:**

Jie Li, MD, PhD

Assistant Professor of Dermatology and Cell Biology

Department of Dermatology & Cutaneous Surgery

Department of Cell Biology and Anatomy

University of Miami School of Medicine

1600 NW 10th Avenue, RMSB 2049, Miami, FL 33136

Phone: 305-243-3365, Fax: 305-243-6191

Email: jli@med.miami.edu

Key words: FTA, Non-Invasive, Electric Magnetic Field, Wound, Reepithelialization

ABSTRACT

It has been well known that very small electric currents produce a beneficial therapeutic result for wounds. However some of the drawbacks which have hindered its clinical application may be its invasive nature and lack of well controlled studies and mechanisms of action. In this study, we evaluated the effects of a non-invasive electric magnetic field device, Field Therapy Accelerator (FTA), on cell migration and proliferation. Two epithelialization models, *in vitro* and *in vivo*, were used. Initial findings using *in vivo* porcine second-degree burn model suggested that exogenous electric magnetic fields can stimulate epithelialization. Further *in vitro* analyses with human skin keratinocyte cultures clearly demonstrated that the FTA has a very strong effect on accelerating keratinocyte migration and a relative weaker effect on promoting keratinocyte proliferation. In addition, the effects of FTA on cell migration and proliferation seem keratinocyte specific with no such effects on dermal fibroblasts. This study suggests that non-invasive electric magnetic field accelerates wound reepithelialization through a mechanism of promoting keratinocyte migration and proliferation.

INTRODUCTION:

Wound healing is a dynamic process and involves numerous cell types, their chemical mediators, and the surrounding extracellular matrix [1]. It is an orderly and progressive pattern that can be divided into three overlapping phases – inflammatory, proliferative, and remodeling.

Reepithelialization takes place in the proliferative phase to restore the epidermis following skin injury. It involves the migration, proliferation, and differentiation (stratification) of keratinocytes as well as the reconstitution of the basement membrane. At the same time, fibroblasts proliferate, migrate into the wound and, later, produce new collagens and other matrices to repair the wounded dermis.

Keratinocyte migration is an early event during wound reepithelialization. Keratinocytes begin migrating from the free edges of a wound, and residual adnexal structures in partial-thickness wounds, within 24 hours after injury. Reepithelialization also involves increased proliferation of keratinocytes located behind the migrating cells of the front tongue, which ensures an adequate supply of cells to migrate and cover the wound. When migration ceases (possibly due to contact inhibition) keratinocytes re-attach themselves to the underlying substratum, reconstitute the basement membrane that connects the neo-epidermis to regenerated dermis, and resume the process of terminal differentiation to generate a new, stratified epidermis.

Wounded skin has been shown to generate physiological electric currents [2, 3]. For more than three decades it has been well known that very small exogenously applied electric currents produce a beneficial therapeutic result for wounds [4]. It was first demonstrated by Dr. Robert Becker's group that by inserting an electrode on each side of a bone nonunion and passing a weak electric current, the fracture would fuse [5].

It has been demonstrated *in vitro* that an applied direct current (DC) electric field directs the migration of keratinocytes toward the negative pole [6, 7], exhibiting galvanotaxis. Although these imposed electric fields have a strong influence on directed migration, they have little influence on the net speed of migration [7], which suggests that the cellular mechanisms involving the direction and speed of movement of keratinocytes are independent of one another. Dermal fibroblasts, in contrast, have been shown not to exhibit galvanotaxis in electric fields of physiologic strength [8]. It has been suggested that they lack the specific signaling pathways used in a galvanotactic response, and instead rely solely on chemotactic factors.

Exogenous extremely low frequency fields applied in fixed juxtaposition to their target tissues (animals and cells of eukaryote and prokaryote origins) have been found to initiate mitogenesis-related signals [9]. On the other

hand, in an *in vitro* study on epidermal explant cultured at an air-liquid interface, low frequency pulsed electrical current changed the balance of proliferation and differentiation in the keratinocytes significantly in favor of differentiation, and in fact decreased the cells' migration and proliferation [10].

The use of invasive electromagnetic therapy for bones and nerves has been widely accepted as beneficial for the patients [4, 11, 12, 13, 14, 15, 16, 17]. However, most of the existing *in vivo* studies focus on animals, not humans. There have been very few electromagnetic field studies of skin wounds *in vivo* in humans, mostly due to a reluctance of researchers to test this highly theoretical and invasive approach.

Non-invasive electromagnetic therapy machines have emerged recently, including SofPulse®, Diapulse®, and the Curatron® 2000XP. However, the research behind these products has mostly been clinical with very few well controlled laboratory mechanistic studies. In this study, we evaluated the effects and potential mechanisms of a newly developed non-invasive electric magnetic field device, the Field Therapy Accelerator (FTA, Advatech), on skin wound repair, using an *in vivo* pig model and *in vitro* cell cultures of human keratinocytes and fibroblasts.

MATERIALS AND METHODS

Induced Electromagnetic Field by FTA:

Advatech's technology, FTA, produces a magnetic field which in turn induces an electric current in the tissue without the need of inserting electrodes into the tissue. It is able to generate a direct current (DC) like pulse of voltage followed for a very short time interval by a negative voltage spike (Figure 1). The DC portion of the electric signal makes up 90% of the signal, or duty cycle=90%; that is, the DC part of the treatment which transports charge is active 90% of the time of the treatment and the reversed electric field, which retards transport, is active only 10% of the time.

In Vivo Pig Study:

Experimental Animals: Pigs were used as our experimental animal since their skin is anatomically and physiologically similar to humans and is considered an excellent tool for the evaluation of therapeutic agents [18]. There is a strong correlation between pig and human wound healing studies. For these studies we used a well defined second-degree wound healing porcine model [19, 20]. Two young female specific pathogen free (SPF: Ken-O-Kaw Farms, Windsor, IL) pigs weighing 25-30 kg were kept in house for two weeks prior to initiating the

experiment. The animals were fed a basal diet *ad libitum* and housed individually in our animal facilities (meeting USDA compliance) with controlled temperature (19-21°C) and lights (12h/12h LD).

Burn Wounding Technique: The animals were clipped with standard animal clippers on the day of the experiment. The skin on the back and both sides of the animals was prepared for wounding by washing with a non-antibiotic soap and sterile water. Antiseptics were not used because of their potential effects on the healing process. The animals were anesthetized and five specially designed cylindrical brass rods weighing 358g each were heated in a boiling water bath to 100°C. A rod was removed from the water bath and wiped dry before it was applied to the skin surface to prevent water droplets from creating a steam burn on the skin. The brass rod was held at a vertical position on the skin for six seconds, with all pressure supplied by gravity, to make a burn wound 8.5 mm diameter x 0.8 mm deep. Immediately after burning, the roof of the burn blister was removed with a sterile spatula. The burn wounds were made approximately 2 cm from each other. Aighty-eight burn wounds were made on the anterior two-thirds of each animal.

FTA Treatments: Burn wounds were randomly assigned to one of the following treatment groups: 1) active magnetic field or 2) sham control (untreated air exposed). Wounds were treated once per day for the first five days with the electric magnetic field apparatus for 1 1/2hrs. The average electric field strength at the pig's skin was 1.2 mV/cm at a frequency of 980 Hz with a duty cycle of 90%.

Epidermal Epithelialization Assessment: Beginning on Day 8 after wounding (Day 0), and each day thereafter until all wounds were 100% completely epithelializedzed, five burn wounds and the surrounding normal skin from each treatment area per pig were excised using an electrokeratome. Any specimens that were not excised intact were discarded. The excised wounds and the surrounding normal skin were incubated in 0.5 M NaBr for 24 hours at 37°C. After incubation the specimens were separated into epidermal and dermal sheets. The epidermis was examined macroscopically for defects in the area of the burn wounds. Epithelialization was considered complete (healed) if no defect(s) were present; any defect(s) in the wound area indicated that healing was incomplete. The epidermal sheet was placed on cardboard for a permanent record.

***In Vitro* Studies with Cell Cultures:**

Cells and Cell Cultures:

Normal human primary fibroblasts were isolated from neonatal foreskin, grown and maintained in Dulbecco's Modification of Eagle's Medium (DMEM) supplemented with 10% fetal bovine serum (FBS) plus 100 μg/ml penicillin, 100 μg/ml streptomycin and 0.25 μg/ml amphotericin B at 37^0C and 10% CO_2. The FBS concentration was changed to 0.1, 0.5, 1, 2 or 5% for fibroblast migration assays, and 1 or 2% for the proliferation analyses. Normal human keratinocytes were maintained in growth medium of EpiLife with human keratinocyte growth supplement at final concentration of bovine pituitary extract (BPE), 0.2% v/v bovine insulin, 5 μg/ml hydrocortisone, 0.18 μg/ml bovine transferrin, 5 μg/ml human epidermal growth factor and 0.2 ng/ml (Cascade Biologics) plus antibiotics of 100 μg/ml streptomycin and 100 μg/ml penicillin at 37^0C and 5% CO2. Media were changed every 24 hours.

Cell Migration Experiment/Data Analysis:

An *in vitro* incisional wound model was used for the cell migration analyses. Cells were maintained in their growth media in 35-mm culture dishes and grown into confluence. At time 0, a cross-shaped wound gap or cell-free zone, about 52-58 cm^2 in size, was made among confluent monolayer cells in the center of the culture dish, and detached cells were washed off with Phosphate Buffered Saline (PBS) and then replaced with growth medium. The cell cultures were examined at time 0 immediate after wounding and every 24 hours thereafter until cells migrated in and completely filled the gaps. A Zeiss Axiovert 200 inverted microscope with a digital camera was used to capture the images and quantified as described below. The center of the cross (where the two scratch lines meet) was used for the positioning of the gap.

Electric magnetic field treatment: Cell culture dishes of treatment groups were placed on the surface of the device and exposed to the electric magnetic field at the electric field strength of 2.5 mV/cm, duty cycle of 90% and temperatures of 31 ± 2^0C. Cells were treated for 1 hour immediately after wounding and every 24 hours thereafter for a total of 4 days. Control groups received no treatment but were placed in the hood at temperature of 31 ± 2^0C for the same period of time of their treatment counterparts. Each group was studied in triplicates. Keratinocytes were divided into 3 groups: Group 1 was treated at frequency of 980 Hz (cycles/second). Group 2 was treated at

frequency of 2080 Hz. Group 3 received no treatment and was used as the control. Fibroblasts were divided into two groups, no treatment control group, and treatment group treated with EMF at frequency of 2080 Hz. We used only 2080 Hz for fibroblast experiment since earlier experiments of keratinocyte migration showed that EMF at 2080 Hz had stronger stimulating effect.

Quantification: Cell migration was quantified by the time and percentage of the wound gap covered by the cells that migrated in from the wound edges subsequently filling the gap. AxioVision 3.0 image analysis software was used to measure the gap area. Each of the gap area was analyzed by two investigators independently. Since each treatment was carried out in triplicates, a total of 6 measurements were obtained for each treatment. The percentage of gap filled (*PGf*) was calculated as $PGf = (1 - At/A0) \times 100$, where At is the gap area at time t, A0 is the gap area at the time 0 immediate after scratch wounding (Figure 2). Finally, one-way analysis of variance (ANOVA) followed by un-paired Student T-test was used for statistical analysis of the *PGf* values. A P value ≤ 0.05 was considered significant. The results were graphed as a function of time elapsed versus *PGf* to compare changes of the treatment groups relative to the untreated controls. A high *PGf* value indicates a strong effect on cell migration.

Proliferation Experiment/Data Analysis:

Cell proliferation analysis: In 35-mm cell culture dishes 1.0×10^5 keratinocytes and fibroblasts each were initially plated for their respective experiments. Cells were divided into treatment and control groups in triplicates for each day. The media for all of the dishes were changed right before each treatment. The cells were plated 12 hours before the first treatment (day 0). Cell counts were made at days 1, 2, 3, 5, and 7 for keratinocytes and days 1, 2, 3, and 5 for fibroblasts. The cells were detached from the dishes with 0.05% trypsin and 0.53 mM EDTA solution and counted using the dye-exclusion hemacytometer method.

EMF treatment: The treatment groups were exposed to the FTA at frequency of 2080 hz, electric field strength of 2.5 mV/cm, and duty cycle of 90% at temperatures of 31 ± 2^0C for the duration of one hour per treatment. Treatments were administered every 24 hours afterwards until day 5 (fibroblasts) or day 7 (keratinocytes). The control groups received no treatment but were placed in the hood at temperature of 31 ± 2^0C for the same period of time of their treatment counterparts.

Quantification: One-way analysis of variance followed by un-paired Student T-test was used for statistical analysis. P value ≤ 0.05 was considered significant. The results were graphed as a function of time elapsed versus total number of cells to compare changes of the treatment groups relative to the untreated controls.

RESULTS

FTA accelerates skin epithelialization *in vivo*:

The electric magnetic field appeared to accelerate the rate of epithelialization of second-degree burn wounds as compared to untreated air exposed (Table 1).). In this study analyzing 2 animals, 10 wounds per treatment group per time point, the treated group demonstrated 100% reepithelialization at least 2 days before 100% reepithelialization of the untreated group. The EMF initiated complete epithelialization at Day 11, when wounds treated were 10% healed (completely epithelialized) as compared to control wounds (untreated), which remained at 0% healed. We also observed a 90% increase in complete epithelialization as compared to control wounds on day 12. On day 13 wounds treated with the electric magnetic field were 100% healed and only 50% of the wounds from the untreated group were healed on this day.

FTA strongly promotes keratinocyte migration:

Since the preliminary *in vivo* pig study showed promoting effects of FTA on the wound reepithelialization, we sought to understand the potential mechanism involved by *in vitro* studies of human cell cultures. We hypothesized that FTA influences the wound reepithelialization through promoting cell migration and/or proliferation. As the first step, we tested the effects of FTA on cell migration in an *in vitro* incisional wound model with normal human keratinocyte. Significantly accelerated cell migration in both treated groups was observed compared with the non-treated control group (Figures 3 and 4, Table 2A and 2B). In the group 2 treated with higher frequency of 2080 cycles/second, electric field strength at 2.5 mV/cm and duty cycle of 90%, dramatically increased gap fillings were seen beginning at day 3 after wounding compared with both group 1 and control ($P<0.001$). The wound gaps completely filled 6 days after wounding, 3 days earlier than other two groups ($P < 0.001$). Compared with control group, there is also significantly increased cell migration in the group 1 treated with lower frequency at 980

cycles/second at days 4 ($P<0.05$), 5 and 6 ($P < 0.001$). It should be noted that for group 1 there was some initial difficulty in maintaining the control temperature within the target of $31\pm2^{0}C$.

FTA slightly increases keratinocyte proliferation:

We next analyzed the effects of FTA on keratinocyte proliferation. No significant effect was identified in the earlier stage of the treatment (day 1-4). Significant increases ($P < 0.01$) in keratinocyte proliferation were observed in treatment group (at frequency of 2080 cycles/second, electric field strength of 2.5 mV/cm and duty cycle of 90%) after 5 and 7 days of treatment (Figure 5, Table 3). However, the effects were not very dramatic as compared to the cell migration (12.5% and 7.2% mean difference between control and treatment group cell counts for days 5 and 7, respectively).

FTA has no significant effect on fibroblast migration or proliferation:

To evaluate whether FTA has the similar effects on fibroblasts, we performed cell migration analysis using the *in vitro* incisional wound model with human primary fibroblasts cultured in DMEM at different FBS concentrations of 0.1%, 0.5%, 1%, 2% and 5%. Both treated and non-treated control groups completely filled the wounding gap after 4 days. To our surprise, the EMF treatment did not show any significant stimulating effect on fibroblast migration (Figure 6, Table 4). Subsequent 5-day experiments of cell proliferation analysis, at FBS concentration of 1% and 2%, showed that FTA device had no significant effect on fibroblast proliferation either (Figure 7, Table 5).

Discussion

There have been several theories on the mechanisms of electric field influence on keratinocytes. One involves the lateral electrophoresis and local clustering of membrane ion channels (such as Ca2+ channels) that increases local fluxes of ions, possibly inducing the cell to form local lamellipodia. Another theory involves the shift in the resting membrane potential between the positive and negative pole sides of the cell, leading to a change in the open probability of the channels that can change the local ion concentrations.

There are a few published reports on the biological effects of electric magnetic field on tissues as mentioned earlier in the introduction. However, those studies were performed with the invasive devices and most with animals or tumor cells. To our knowledge, the current study is the first to examine the potential effects and mechanisms that a non-invasive EMF exerts on cutaneous wound using both an *in vivo* pig wound model and *in vitro* normal human keratinocyte and fibroblast cultures. The preliminary *in vivo* study of a pig burn wound model revealed that the non-invasive EMF device, FTA, appeared to accelerate the rate of reepithelialization of second-degree burn wounds. The further *in vitro* analyses clearly demonstrated that the FTA has very strong effect on accelerating keratinocyte migration and a weaker effect on promoting keratinocyte proliferation. In addition, the effects of FTA on cell migration and proliferation seem keratinocyte specific-with no such effects on dermal fibroblasts.

Due to the various and sometimes ambiguous parameters used in the electrical stimulation experiments, it has been difficult to compare and make solid conclusions over different studies. After an evaluation of numerous published studies, Reich and Tarjan [21] suggested two standard electrical parameters to render electrical stimulation studies more suitable for comparison – average spatial current density and equivalent duty cycle, which define the treatment in terms of the dosage and dose rate per unit area during the treatment. The current density is the best indicator of the electrochemical effects for invasive EMF, since voltages change with distance from the electrodes, while current stays the same throughout the sample. The duty cycle is also extremely important, as it expresses the equivalent percent of time the current is being delivered. These factors are easily interpreted and compared in studies of time-varying currents (exponentially decaying, pulsatile, or sinusoidal). Compared to the others, pulsed electrical stimulation yields superior wound healing, as it allows higher current densities without tissue irritation or burning. One of the main drawbacks of these treatments are that they are invasive and require delivery dressings or electrodes to be in direct contact to the wounded area.

The Advatech device FTA produces a typical electric field that is much more powerful than previous reported non-invasive electromagnetic devices. This is accomplished by increasing both the average electric field strength from typical values of 0.5 mV/cm or less to 2.5 mV/cm and by increasing the duty cycle (on time) from 4% to 90%. The product of these two ratios (2.5/0.5= 5 and 90/4=22.5) yields more than a hundred fold increase.

The average field strength produced by FTA, 2.5 mV/cm, is still much lower than the 100 mV/cm tested in some previous invasive studies. However, the same treatment parameters and effects of invasive electromagnetic therapy do not seem to extrapolate to non-invasive therapies. Three factors may account for this. First, the field generated in non-invasive therapy is an *induced* field, without specific polarized electrodes acting as focal points of field strength. Second, without specific polarities present, the native ion species in the cellular environment are not aggregated to electrodes. Lastly, there is a voltage drop between the electrodes and along the electromagnetic field lines in invasive treatments [22, 23], while the voltage is relatively constant throughout the sample in non-invasive treatments.

Our data suggests that the non-invasive EMF treatment accelerates wound reepithelialization through a mechanism of promoting keratinocyte migration and proliferation. The study showed that EMF has no such effects on dermal fibroblasts. However, EMF might have stimulating effects on fibroblasts at presence of certain growth factor, cytokine, integrin receptor or extracelluar matrix. It is also possible that EMF influences fibroblasts in other process important to wound healing, such as production of extracellular matrices. Future studies with cDNA microarrays and RT-PCR analysis to examine gene expression patterns will help to shed light on the molecular basis of these effects. In addition, although a trend in reepithelialization of second-degree burns was seen in pig study, additional animals are needed to substantiate this claim. Further controlled *in vivo* investigations on the use of non-invasive EMF for various types of wounds, e.g. acute and chronic, are warranted.

References:

1. Li J and Kirsner RS. Wound Healing, In: Surgery of the Skin, Robinson JK, Hanke CW, Sengelmann RD and Siegel DM eds., Elsevier Inc., 97-115, 2005.

2. Jaffe LF, Vanable JW. Electrical fields and wound healing. Clin Dermatol 1984; 2(3):34-44.

3. Illingworth CM, Barker AT. Measurement of electrical currents emerging during the regeneration of amputated fingertip in children. Clin Phys Physiol Meas 1980; 1:87-89.

4. Davis SC, Ovington LG. Electrical stimulation and ultrasound in wound healing. Dermatologic Clinics 1993; 775-78.

5. Bassett CAL, Pawluck RJ, Becker R. Effects of electric currents on bone formation in vivo. Nature 1964; 204:652.

6. Fang KS, Farboud B, Nuccitelli R, Isseroff RR. Migration of human keratinocytes in electric fields requires growth factors and extracellular calcium. J Invest Dermatol 1998; 111:751-756.

7. Nishimura KY, Isseroff RR, Nuccitelli R. Human keratinocytes migrate to the negative pole in direct current electric fields comparable to those measured in mammalian wounds. J Cell Science 1996; 109:199-207.

8. Sillman AL, Quang DM, Farboud B, Fang KS, Nuccitelli R, Isseroff RR. Human dermal fibroblasts do not exhibit directional migration on collagen I in direct-current electric fields of physiological strength. Experimental Dermatology 2003; 12:396-402.

9. Beech JA. Bioelectric potential gradients may initiate cell cycling: ELF and Zeta potential gradients may mimic this effect. Bioelectromagnetics 1997; 18:341-348.

10. Hinsenkamp M, Jercinovic A, Graef C, Wilaert F, Heenen M. Effects of low frequency pulsed electrical current on keratinocytes in vitro. Bioelectromagnetics 1997; 18:250-254.

11. Bassett CAL, Pawluck RJ, Pilla AA. Augmentation of bone repair by inductively coupled electromagnetic fields. Science 1974; 184:575-577.

12. Bassett CAL. Fundamental and practical aspects of therapeutic uses of pulsed electromagnetic fields (PEMFs). Crit Rev Biomed Engineer 1989; 17:451-529.

13. Kerns JM, Lucchinetti C. Electrical field effects on crushed nerve regeneration. Exp Neur 1992; 117:71-80.

14. McLeod KJ, Rubin CT. The effect of low frequency electrical fields on osteogenesis. J Bone Joint Surgery 1992; 74A:920-929.

15. Sisken BF, Walker J, Orgel M. Prospects of clinical applications of electrical stimulation for nerve regeneration. J Cell Biochem 1992; 52:404-409.

16. Zienowicz RJ, Thomas B, Kurtz W, Orgel M. A multivariate approach to the treatment of peripheral nerve transaction injury: The role of electromagnetic field therapy. Plastic Reconstruct Surg 1991; 87:122-129.

17. Mertz PM, Davis SC, Cazzaniga AL, Cheng K, Reich JD, Eaglstein WH. Electrical stimulation: Acceleration of soft tissue repair by varying the polarity. Wounds 1993; 5(3):153-159.

18. Sullivan TP, Eaglstein WH, Davis SC, Mertz PM. The pig as a model for human wound healing. Wound Rep Reg 2001; 9:66-76.

19. Davis SC, Mertz PM, Eaglstein WH. Second degree burn healing: The effect of occlusive dressings and a cream. J Surg Res 1990; 48:245-248.

20. Mertz PM, Davis SC, Franzén L, Uchima FD, Pickett MP, Pierschbacher MD, Polarek JW. Effect of an RGD peptide-containing artificial matrix on epithelial sheet migration and experimental second-degree burn wound healing. J Burn Care and Rehabilitation 1996; 17(3): 199-206.

21. Reich JD, Tarjan PP. Electrical stimulation of skin. International Journal of Dermatology 1990; 29:395-400.

22. Reich JD, Cazzaniga AL, Tarjan PP, Mertz PM. The reporting and characterization of exogenous electric fields. Electromagnetics in Biology and Medicine 1991; 355-360.

23. Cheng K, Tarjan PP, Thio YC, Mertz PM. In vivo 3-D distributions of electric fields in pig skin with rectangular pulse electrical current stimulation (RPECS). Bioelectromagnetics 1996; 17:253-262.

Legend:

Table 1: The numbers of wounds healed (completely epithelialized) were tabulated and divided by the total number of wounds sampled per day and multiplied by 100 to give a percent of wound completely epithelialized. Since this is a preliminary study, statistical analysis was not performed.

Table 2: Summary of % gap filled for keratinocyte migration assay.

1A shows the results of % gap filled for keratinocyte migration assay. First column is the days after wounding. Right columns are the measure of % gap filled expressed as Mean value ± Standard Error of Measurement (Std Error). 1B shows the P values for keratinocyte migration assay. Since the keratinocytes of treatment group 2 completely filled the gap at the day 6, only P values for the day 1-6 were listed. Note: G1, treatment group1; G2, treatment group 2; and Ctr, non-treated control.

Table 3: This table is the summary of cell counts for keratinocyte proliferation analyses.

First column is the days of the treatment. Right columns are the measure of the cell counts expressed as Mean ± Std Error. P value is shown when it is significant ($P<0.05$).

Table 4: This table is the summary of % gap filled for fibroblast migration assay.

First column is the days after wounding. Right columns are the measure of % gap filled expressed as Mean ± Std Error for the control and treatment groups. P values are not shown, since all P values are >0.05.

Table 5: This table is the summary of cell counts for fibroblast proliferation analysis. First column is the days of the treatment. Right columns are the measure of the cell counts expressed as Mean ± Std Error. P values did not show, since all P values are >0.05.

Figure 1: FTA electric magnetic field device. Left. A graphical demonstration that FTA generates a direct current (DC) like pulse of voltage followed by a very short time interval of a negative voltage spike. The DC part of the

treatment (DC on), which transports charge, is active 90% of the time and the short reversed electric field (Reverse Voltage), which retards transport, is active only 10% of the time. Right. Three 35-mm tissue culture dishes held in a 100-mm dish were placed on the top of the FTA device for the treatment. The area of round-shaped electric magnetic field is slightly larger than that of the 100-mm dish.

Figure 2: This figure demonstrates the method of cell migration assay using an *in vitro* incisional wound model. Left: At time 0, a cross-shaped wound gap or cell-free zone was made among confluent monolayer cells in the center of the culture dish. The center of the cross (where the two of scratch lines meet) was used for the positioning of the gap. Right: Cell migration was quantified by the percentage of the wound gap covered by the cells that migrated in and filled the gap. The percentage of gap filled (*PGf*) was calculated as $PGf = (1 - A_t/A_0) \times 100$, where A_0 is the gap area at the time 0 immediate after scratch wounding (left), and A_t is the gap area at time t (right).

Figure 3: This figure shows some selected microscopic observations of wound gap filled in the keratinocyte migration assay. Note top panels: G1, treatment group 1; center: G2, treatment group 2; and bottom: Ctr, non-treated control group. Columns: left, day 0; center, day 3; right, day 5.

Figure 4: Effects of electric magnetic field on keratinocyte migration. This figure is a graphical representation of the wound gap filled in treatment groups and non-treated controls. Y-axis shows the percent of gap filled (*PGf*). X-axis shows the days after wounding. Note: blue bar, treatment group 1; red bar, treatment group 2; yellow bar, non-treated controls. Here, the wound gaps filled at the time t (after treatment day 1-9) are presented as a percent of the gap at time 0, at which it is 100%. *PGf*0 at day 0 is not shown. Each bar represents the mean value ± Standard Error of Measurement (Std Error).

Figure 5: Effects of FTA on keratinocyte proliferation. This figure is a graphical representation of keratinocyte proliferation. Y-axis shows the cell number counts. X-axis shows the days of treatment. Note: blue bar, non-treated controls; red bar, treatment group. Here, the numbers indicate the total cell number x 10^4 per dish counted at day 1-7 after treatment. The number at day 0 is the cell number plated. Each bar represents the mean value ± Std Error.

Figure 6: Effects of FTA on fibroblast migration. This figure is a graphical representation of the wound gap fillings. In this experiment, the concentration of FBA is 0.5%. The experiments with 0.1, 1, 2 and 5% FBS showed similar results. Y-axis shows the percent of gap filled. X-axis shows the days of treatment after wounding. Note: blue bar, non-treated controls; red bar, treatment group. Here, the wound gap filled at the time t (after treatment day 1-4) is presented as a percent of the gap at time 0, at which it is 100%. Each bar represents the mean value ± Std Error.

Figure 7: Effects of FTA on fibroblast proliferation. This figure is a graphical representation of fibroblast proliferation. In this experiment, the concentration of FBA is 1.0 %. Y-axis shows the cell number counts. X-axis shows the days of treatment. Note: blue bar, non-treated controls; red bar, treatment group. Here, the numbers indicate the total cell number x 10^4 per dish counted at day 1-5 after treatment. The number at day 0 is the cell number plated. Each bar represents the mean value ± Std Error.

TABLES

Table 1: Epithelialization results*

	D8	D9	D10	D11	D12	D13	D14
Treated	0/10 (0%)	0/10 (0%)	0/10 (0%)	1/10 (10%)	9/10 (90%)	10/10 (100%)	10/10 (100%)
Control	0/10 (0%)	0/10 (0%)	0/10 (0%)	0/10 (0%)	1/10 (10%)	5/10 (50%)	8/10 (80%)

*Data is presented as the number of wound completely epithelialized over the total number of wounds assessed.
( ) Percent of wounds completely epithelialized

Table 2A: Summary of % gap filled for keratinocyte migration assay

	Group 1		Group 2		Control	
Day	Mean	Std Error	Mean	Std Error	Mean	Std Error
0	0	0	0	0	0	0
1	5.68	0.513	10.94	0.466	7.35	0.878
2	10.97	0.503	19.99	0.729	10.57	1.819
3	20.87	1.885	43.50	2.050	15.25	2.426
4	36.23	2.051	75.97	2.230	26.54	4.454
5	58.23	1.224	90.87	1.972	41.10	4.297
6	79.74	0.649	100	0	65.49	1.348
7	89.83	1.228	100	0	83.31	1.449
8	96.43	1.087	100	0	94.33	1.380
9	100	0	100	0	100	0

Table 2B: P values for keratinocyte migration assay

Day	G1 vs G2	G1 vs Ctr	G2 vs Ctr
1	>0.05	>0.05	>0.05
2	>0.05	>0.05	<0.05
3	<0.001	>0.05	<0.001
4	<0.001	<0.05	<0.001
5	<0.001	<0.001	<0.001
6	<0.001	<0.001	<0.001

Table 3: Summary of cell counts for keratinocyte proliferation assay

	Number of Cells ($x10^4$)				
	Control		Treatment		
Day	Mean	Std Error	Mean	Std Error	P
0	10	0	10	0	
1	9.87	0.668	9.45	0.541	
2	13.00	0.510	14.25	0.627	
3	17.88	0.491	18.73	0.680	
5	32.60	0.645	36.68	0.516	<0.01
7	57.26	0.877	61.40	1.194	<0.01

Table 4: Summary of % gap filled for fibroblast migration

Control	Treatment

Day	Mean	Std Error	Mean	Std Error
0	0	0	0	0
1	35.29	2.938	37.50	3.033
2	69.80	2.386	79.59	3.529
3	98.94	0.378	99.30	0.310
4	1	0	1	0

Table 5: Summary of Cell Counts for Fibroblast Proliferation Assay

	Number of Cells ($x10^4$)			
	Control		Treatment	
Day	Mean	Std Error	Mean	Std Error
0	10	0	10	0
1	9.87	0.355	9.71	0.254
2	11.71	0.455	11.28	0.384
3	14.67	0.315	14.39	0.562
5	17.38	0.908	17.1	0.548

FIGURES

Figure 1: FTA device treatment

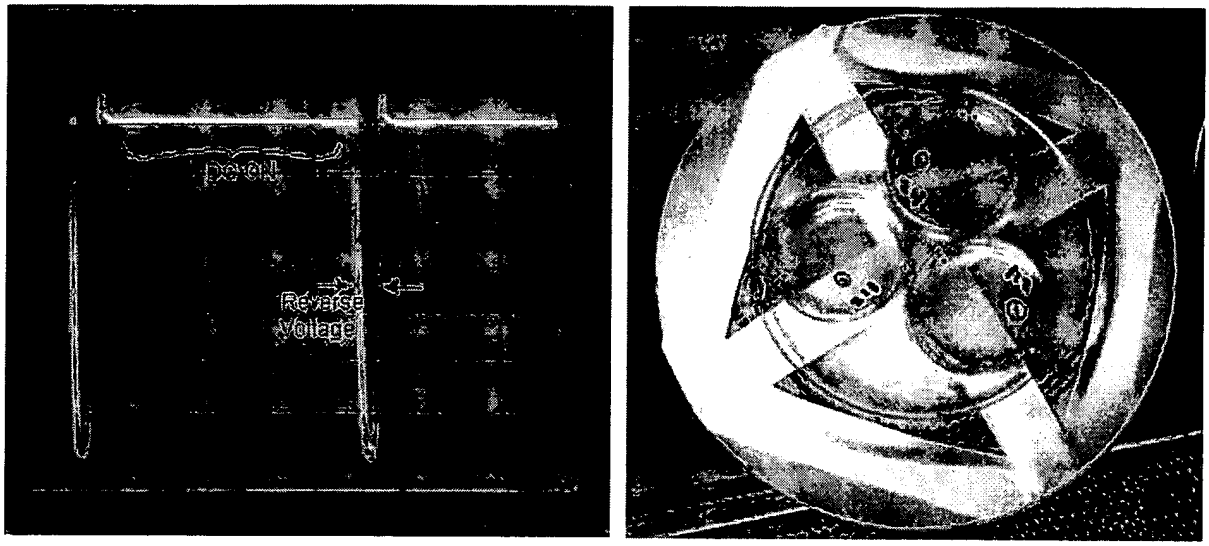

Figure 2: Method of cell migration assay using incisional wound model

A0 **At**

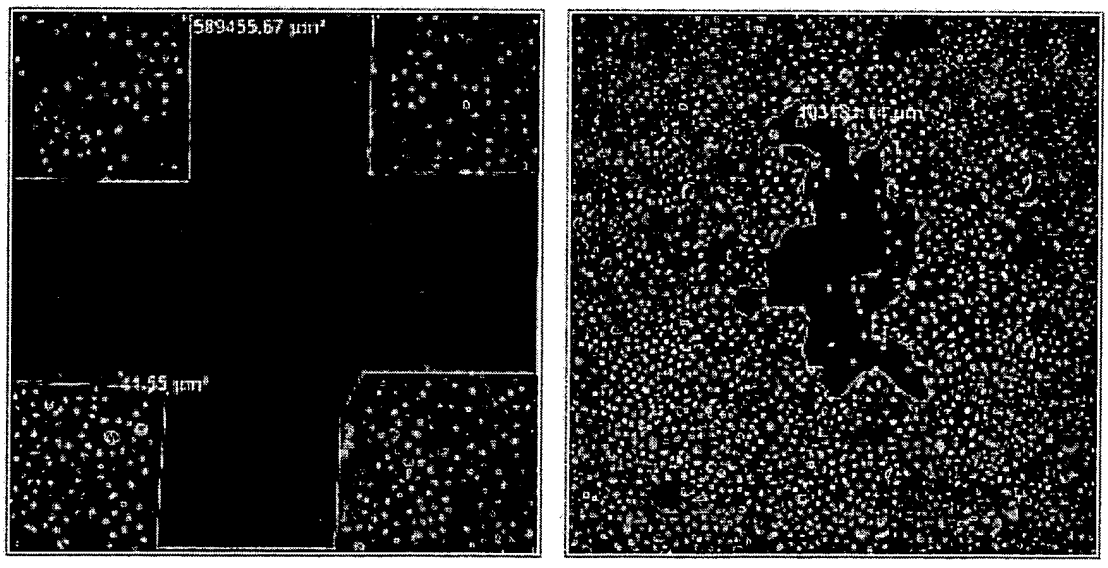

Figure 3: Increased cell migration/gap filling rate with electric magnetic field treatment

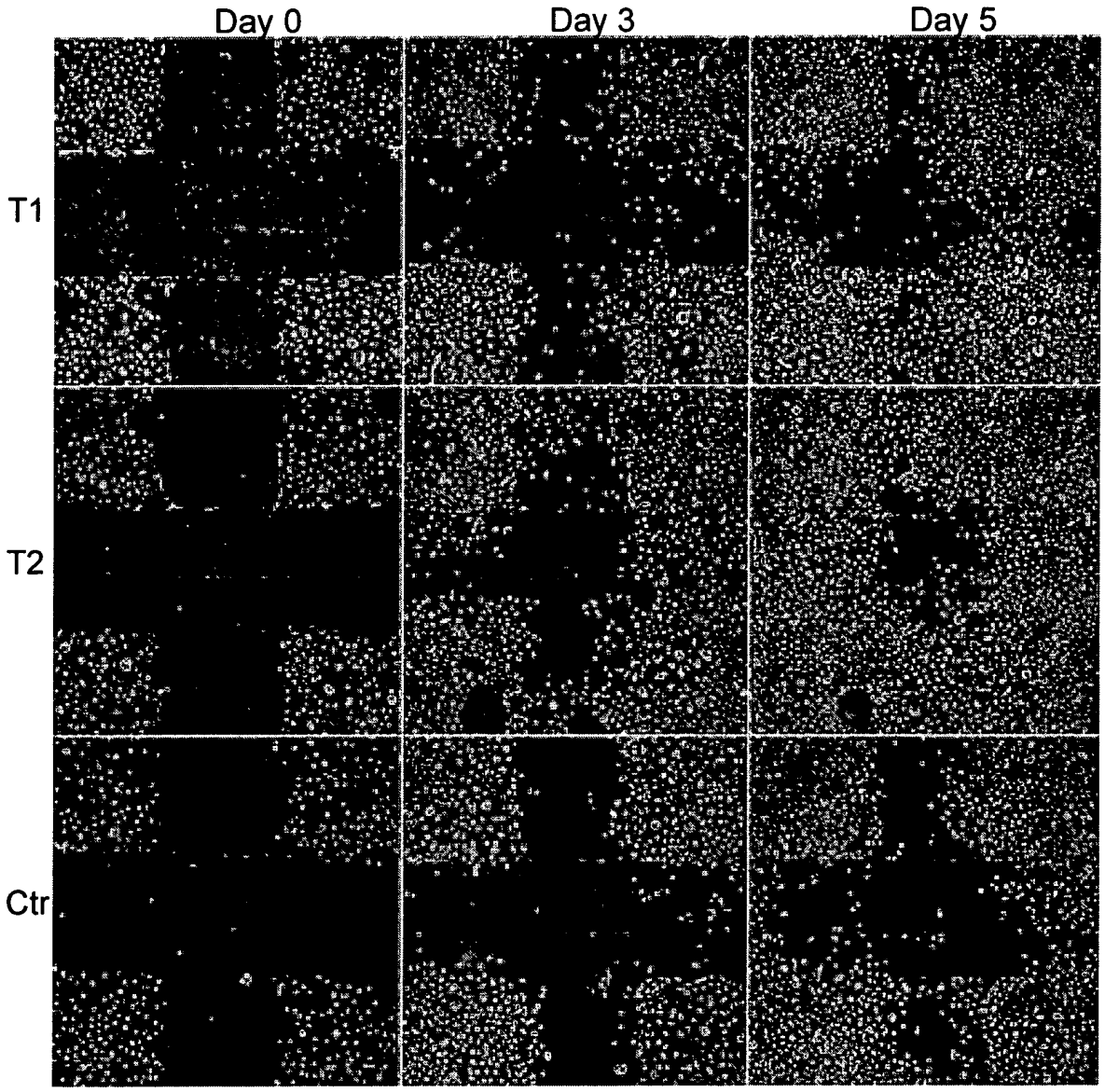

Figure 4: Effects of electric magnetic field on keratinocyte migration

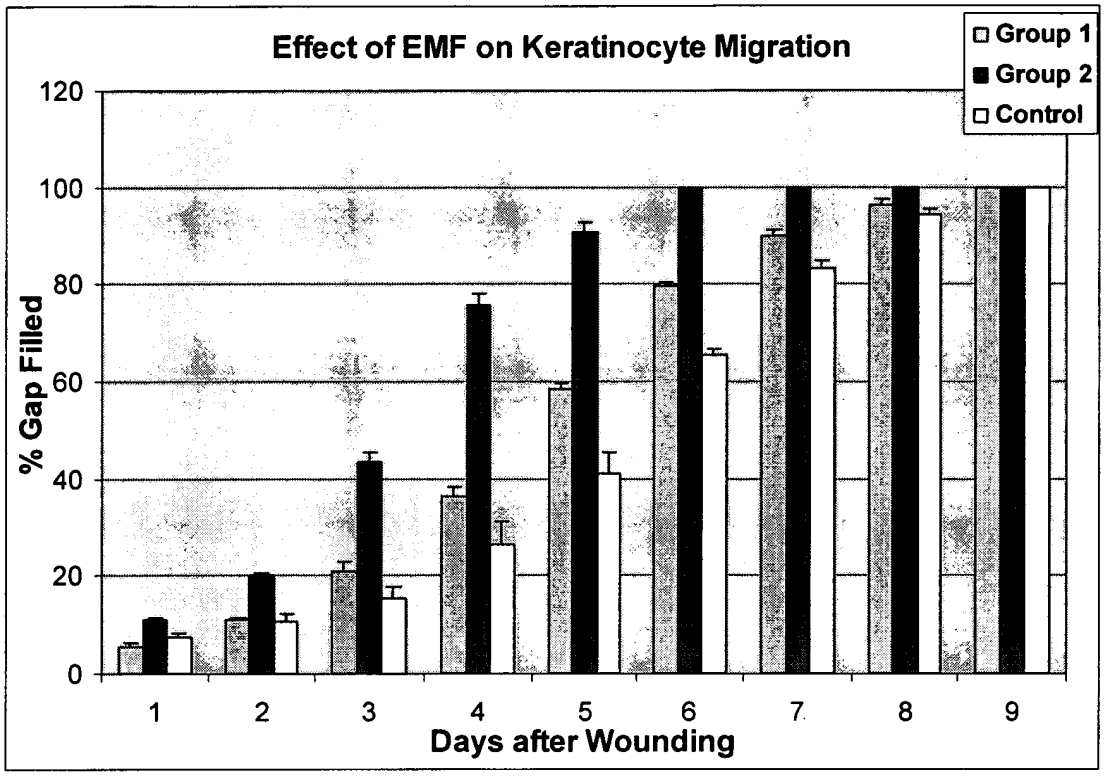

Figure 5: Effects of electric magnetic field on keratinocyte proliferation

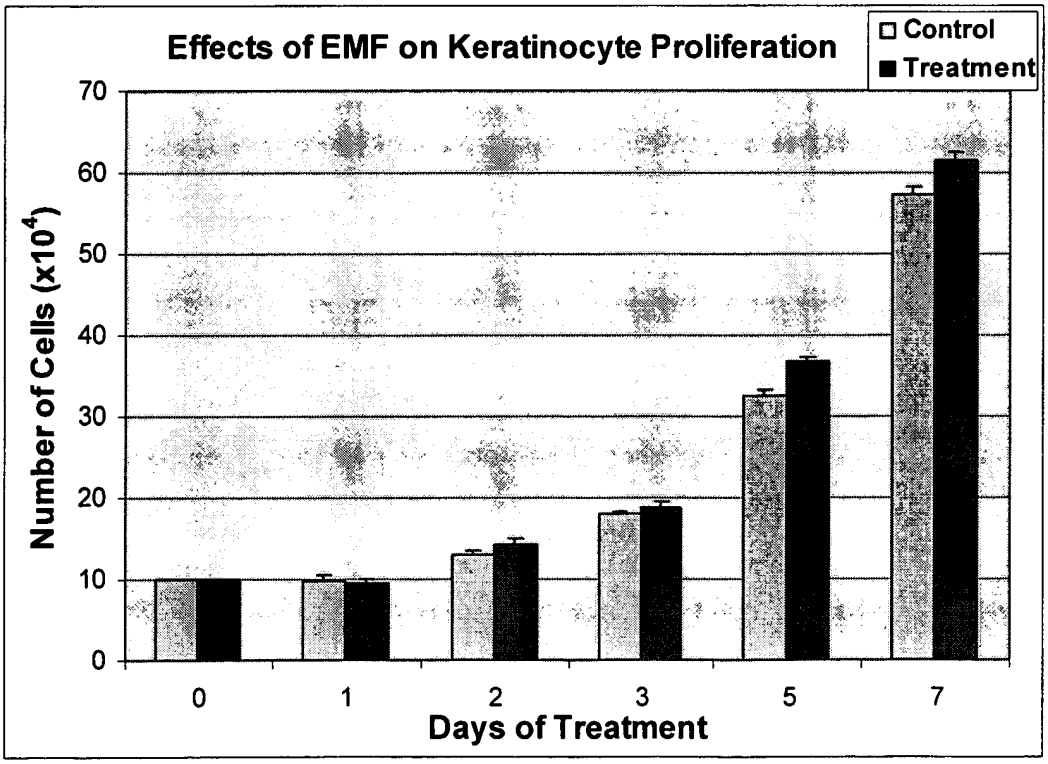

Figure 6: Effects of electric magnetic field on fibroblast migration

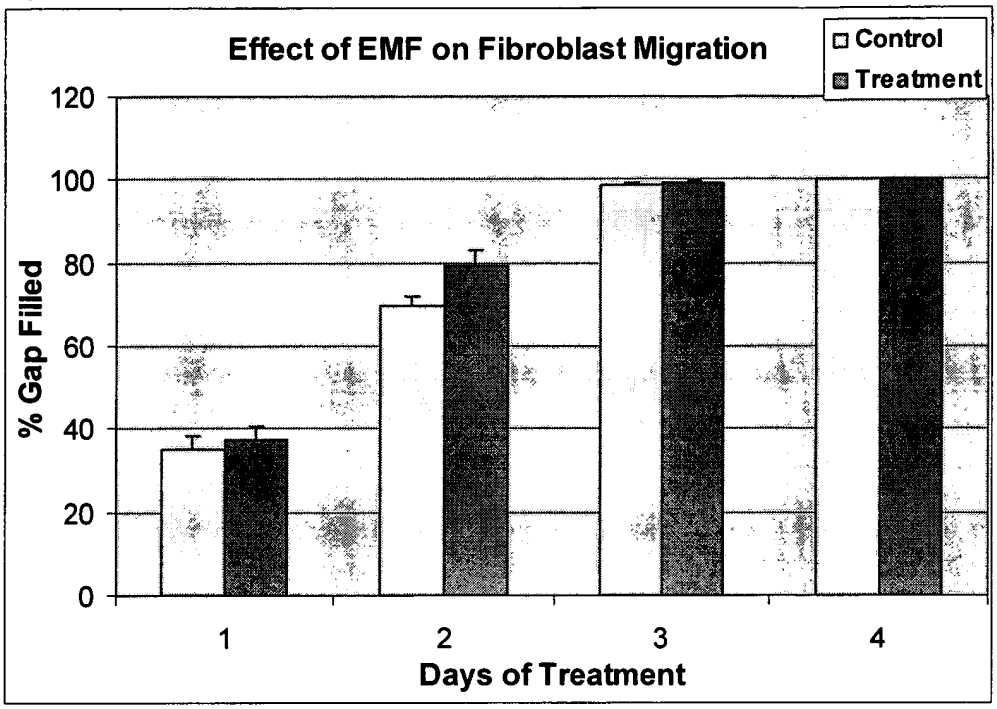

Figure 7: Effects of electric magnetic field on fibroblast proliferation

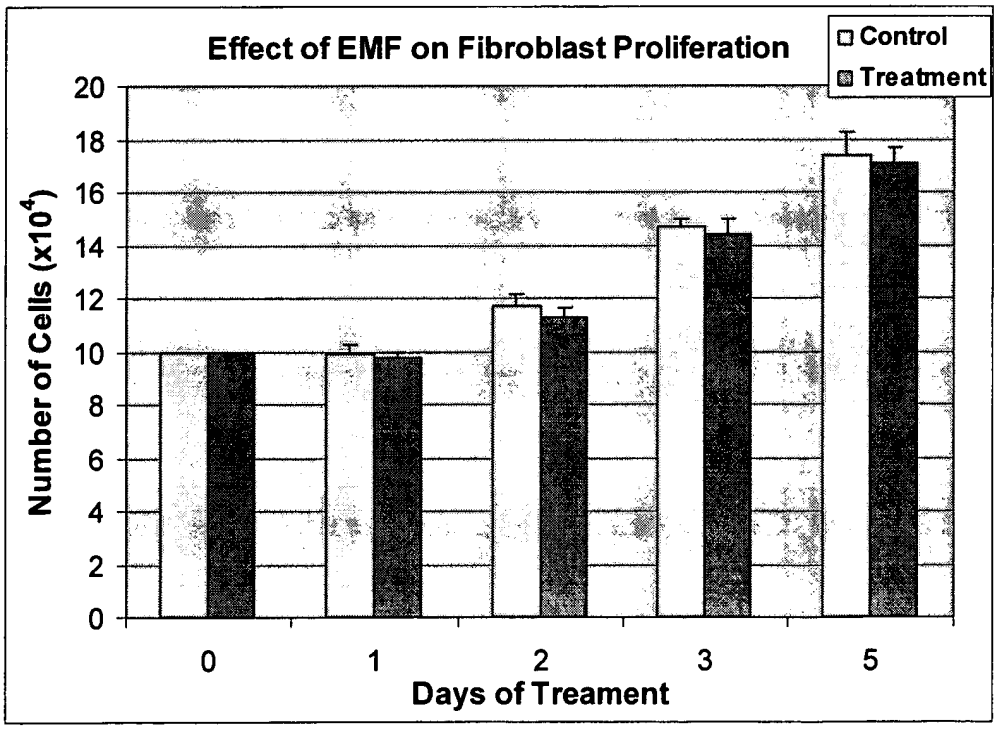

UNIVERSITY OF Miami

SCHOOL OF MEDICINE

Department of Dermatology and Cutaneous Surgery

Skin Biology Research Laboratory

RT-PCR ANALYSIS REPROT

May 28, 2006

INVESTIGATORS AND TESTING FACILITY

University of Miami School of Medicine
Department of Dermatology & Cutaneous Surgery
1600 N.W. 10th Ave., RMSB 2049A
Miami, FL 33136

Jie Li, MD, PhD
Assistant Professor

Ran Huo
Student Research Fellow

Yuqi Jing, PhD
Postdoctoral Research Associate

Juan Chen, MD
Postdoctoral Research Associate

SPONSOR

Advatech Corp.
199 Palm Avenue
Miami Beach, FL 33139

SPONSOR REPRESENTATIVES

Michael Spiegel, Ph.D.

OBJECTIVE

The objective of this study is to verify the microarray data and to examine the mechanisms of stimulatory effect of an electric magnetic field device FTA (Advatech Corp.) on human skin keratinocyte migration in an in vitro incisional wound healing model.

MATERIALS AND METHODS

Cell cultures: Normal human epidermal keratinocytes were maintained in 35-mm cell culture dishes and in a keratinocyte growth medium of EpiLife (Cascade biology) at 37^{0}C and 5% CO_2.

Cell migration Assay: keratinocytes were maintained in growth media and grow into confluent. At time 0, a cross-shaped wound gap or cell-free zone was made among confluent monolayer cells in the center of the culture dish, and detached cells were washed off with PBS and then replaced with growth medium.

Electric magnetic field treatment: 2 treatment groups and each in triplicates. Cells were treated for 1 hour immediate after wounding.

1. Group 1 - at frequency of 2080 cycles/second, electric field strength of 20mV/cm, and duty cycle of 90%.
2. Control: no treatment.

RNA isolation and RT-PCR reaction:

- Total RNAs were isolated from samples using Qiagen RNA isolation kit.
- 4 genes were selected for RT-PCR analyses based on the earlier microarray data.
- Primers: human-specific primers were developed according to human sequences from Genbank or literature (Table 1).
- Reverse transcription and polymerase chain reaction (RT-PCR): RT-PCR reactions were carried out with RT-PCR kit (Qiagen). Reactions were performed for each treatment in duplicate (Figure 1).

Table 1. Primers used in PCR reactions

PRIMER		Sequence	PCR product length (bp)	source
SLC1A7	Fw	GGA GAC TGC ATA GGC AAC TAG	420	GI: 33875686
	Rv	GCA CTG GGA ACA CAT TGG TGA		
CRK7	Fw	GCA GAG CCT TTC CAT ACC TGT	377	GI: 6717322
	Rv	GCA CTG GGA ACA CAT TGG TGA		
CALD1	Fw	CTG GAA CTC CCG AAG CAA TCA	140	GI: 11008923
	Rv	CAG CCA AAT CTA CTC CTC CCA		
HOXC8	Fw	GTG GTG CAA TAT CCC GAC TGT	272	GI: 45580721
	Rv	CCT TCG GTT CTG GAA CCA GAT		
β-Actin	Fw	GTG GGG CGC CCC AGG CAC CA	540	GI: 28251
	Rv	CTC CTT AAT GTC ACG CAC GAT TTC		

Note: SLC1A7, solute carrier family 1 (glutamate transporter) member 7; CRK7, CDC2-related protein kinase 7; CALD1, caldesmon 1; HOXC8, homeo box C8

Figure 1: RT-PCR thermal cycles

For CRK7, CALD1 and β-actin

-Reverse transcription, 30 min at 50°C
-Denaturation, 15 min at 95° C
-34 PCR cycles:

- denaturation: 94°C for 30 sec
- annealing: 65°C for 1 min
- extension: 72°C for 90 sec

-Final extension for 8 min at 72°C

For HOXC8 and β-actin

-Reverse transcription, 30 min at 50°C
-Denaturation, 15 min at 95° C
-36 PCR cycles:
- denaturation: 94°C for 30 sec
- annealing: 50°C for 1 min
- extension: 72°C for 90 sec

-Final extension for 8 min at 72°C

Gel electrophoresis:
RT-PCR products were run on 2% agarose gel in duplicate. As an internal control, β-actin (a house keeping gene) RT-PCR products were always combined with the testing RT-PCR products when loading to gel. After running, the gel was stained with ethidium bromide.

Semi-quantitative analysis:
Analysis was performed using Bio-Rad Quantity-One Image gel documentation system and software. The density of each band of SLC1A7, CRK7, CALD1 and HOXC8 was divided by the density of its respective β-actin band for normalization. The resulted value was expressed as the relative intensity. A student t test was used for statistical analysis. P value of ≤ 0.05 is considered significant.

RESULTS:
1. There was a significant increase of the expression of CDC2-related protein kinase 7 (CRK7, figure 2A and 2B, table 2) and of homeo box C8 (HOXC8, figure 3A and 3B, table 3) in FTA treatment group compared with non-treated control group. Both P values < 0.001.
2. Compared with control group, there was no significant change of the mRNA expression of caldesmon 1 (CALD1) could be observed in the treated group (figure4, table 4), $P > 0.05$.
3. The RT-PCR analysis failed to detect the expression of solute carrier family 1 (glutamate transporter) member 7 (SLC1A7).

Figure 2. CRK7 RT-PCR analysis

2A. Ethidium Bromide gel electrophoresis

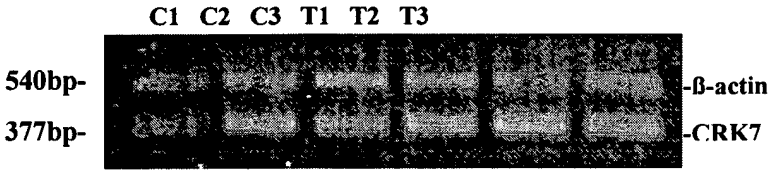

Note: C, control; T, treatment

2B. Relative intensity (mean gray value)

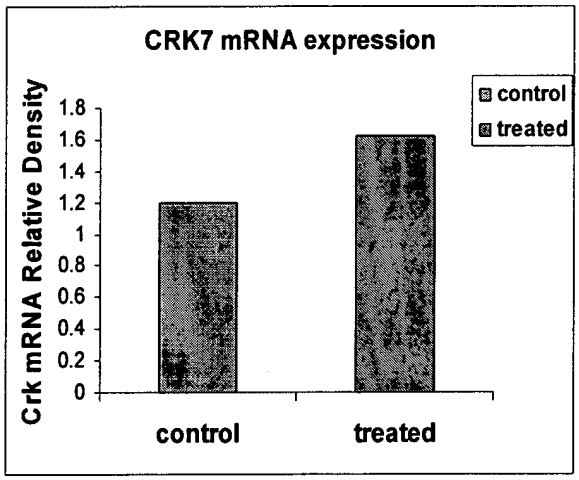

Table 2. CRK7 RT-PCR analysis		
Relative intensity	**Treated**	**Control**
Number	12	12
Minimum	1.252	0.6963
25% Percentile	1.419	0.7538
Median	1.577	1.286
75% Percentile	1.656	1.561
Maximum	2.369	1.700
Mean	1.618995	1.195543
SD	0.33672	0.386035
SErr	0.09720	0.1114
P value	0.000854	

Figure 3. Hoxc8 RT-PCR analysis

3A. Ethidium Bromide gel electrophoresis

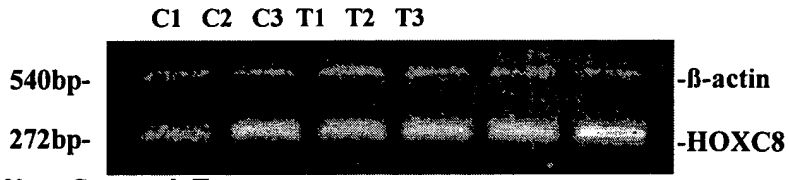

Note: C, control; T, treatment

3B. Relative intensity (mean gray value)

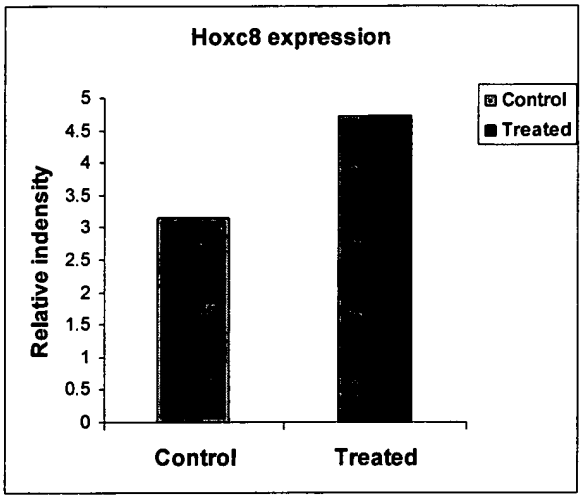

Table 3. Hoxc8 RT-PCR analysis		
Relative intensity	**Treated**	**Control**
Number	12	12
Minimum	4.033	2.357
25% Percentile	4.285	2.766
Median	4.503	2.954
75% Percentile	4.765	3.557
Maximum	6.388	4.364
Mean	4.717907	3.144546
SD	0.687506	0.614168
SErr	0.1985	0.1773
P value	0.000112	

Figure 4. CALD1 RT-PCR analysis

Ethidium Bromide gel electrophoresis

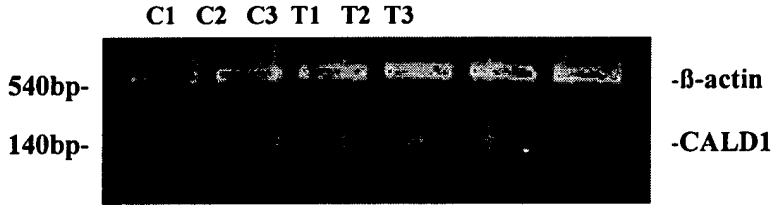

Table 4. CALD1 RT-PCR analysis		
Relative intensity	**Treated**	**Control**
Number	12	12
Minimum	0.2203	0.3562
25% Percentile	0.2937	0.4195
Median	0.5150	0.7495
75% Percentile	0.8181	0.8022
Maximum	0.9630	0.8574
Mean	0.5554	0.6592
SD	0.2779	0.1955
SErr	0.08022	0.05642
P value	0.082456	

Note: SD, standard deviation; SErr, standard error

DISCUSSION:

The RT-PCR analysis data showed that there were increased expression of CDC2-related protein kinase 7 (CRK7, figure 2 and table 2) and of homeo box C8 (HOXC8) after FTA treatment. Both these two genes are the early response genes. It seems reasonable since we isolated RNA from cells after only 1 hour treatment. The homeo box c8 has been shown involved in gene regulation while CDC2-related protein kinase 7 has been indicated in promoting cell migration. Although there were increased expression level of caldesmon 1 and

solute carrier family 1 member 7 genes shown by microarray analysis data, RT-PCR analysis could not detect the significant change for caldesmon 1 and could not detect the expression of solute carrier family 1 member 7.